

Continuous integrated filtration, washing and drying of aspirin: digital design of a novel intensified unit

Francesco Destro* Vivian Wang** Mesfin Abdi** Xin Feng** Erin Wood** Simon Coleman*** Paul Firth***
Alastair Barton*** Massimiliano Barolo* Zoltan K. Nagy****

*CAPE-Lab, Department of Industrial Engineering, University of Padova, Padova, Italy

**Center for Drug Evaluation and Research, Food & Drug Administration, Silver Spring, MD, USA

***Alconbury Weston Ltd, Stoke-on-Trent, UK

****Davidson School of Chemical Engineering, Purdue University, West Lafayette, IN, USA

Abstract: Within the recent modernization of pharmaceutical manufacturing, an important milestone consists in developing enabling technologies for end-to-end continuous production of drug products. Continuous filtration, washing and drying of active pharmaceutical ingredients from mother liquors in upstream manufacturing are critical steps for achieving end-to-end continuous production. In this work, we develop a mathematical model for a novel intensified carousel system capable of continuously filtering, washing and drying a slurry stream into a dry crystals cake. The mathematical model consists of detailed dynamic differential mass, energy and momentum balances, capable of tracking the solvents and impurities content in the cake (critical quality attributes) across the entire carousel. We successfully demonstrate the model features by identifying the probabilistic design space in a simulation study for the isolation of aspirin crystals in the carousel, accounting for model uncertainty through Monte Carlo simulations.

Keywords: Continuous pharmaceutical manufacturing, Mechanistic process modeling, Quality by Design, Design space identification, Chemical Process Control

1. INTRODUCTION

Traditional batch pharmaceutical processing is transitioning to a more continuous production mode, due to the general agreement among practitioners and regulatory bodies on the benefits of continuous manufacturing for process efficiency and product consistency (Lee *et al.*, 2015). Continuous active pharmaceutical ingredient (API) purification after the synthesis section represents a key step in the end-to-end continuous paradigm, as impurities not eliminated here will be transferred down to the drug product. API purification is typically achieved through a train of crystallization, filtration, washing and drying steps. Even though many studies have been conducted on continuous crystallization, investigations on continuous implementations of filtration, washing and drying lag behind, and the continuous integration of purification units is even less explored, both experimentally and computationally.

Filtration, washing and drying unit operations should be designed altogether in an integrated fashion with the support of mathematical models, given the strong interaction among their design and operating parameters. Knowledge-based design is critically important in API manufacturing, as emphasized by the recent interest in enhancing pharmaceutical operation through process understanding, promoted by the US Food & Drug Administration (FDA), e.g. through the Quality-by-Design initiative (FDA, 2004). Nonetheless, in the process and pharmaceutical industries solid/liquid separation is still typically conceived through empirical methodologies and shortcut methods, designing each of the processing steps separately (Tarleton and Wakeman, 2006). Early studies on integrated solid/liquid separation design (Wibowo *et al.*, 2001)

investigate the effect of the crystal size distribution (CSD) of the crystallizer outlet slurry onto the subsequent purification operations employing short-cut methods. Integrated API isolation is considered within a more advanced modeling framework by Benyahia *et al.* (2012). The authors develop a dynamic model of a plant-wide continuous pharmaceutical process, including the isolation section, but their focus is on plant-wide simulation of a specific process, rather than in addressing the current issues in API purification design. Sen *et al.* (2013) provide useful information on the effect of purification operations onto the properties of the drug product through a flowsheet model, built combining hybrid population balances and discrete element method modeling. However, their flowsheet is a digital assembly of unit operation models, and it does not have a physical counterpart that has actually been used for API purification. As such, fundamental phenomena occurring in real plants are not investigated (for example, the washing step is not included in the flowsheet, and the effect of model uncertainty is not considered). Overall, a comprehensive work on detailed mathematical modeling and knowledge-based design for an actual continuous API filtration, washing and drying process is still missing in the literature.

In this study, we develop a comprehensive mechanistic model of a novel carousel system for integrated continuous filtration and washing (Liu *et al.*, 2019), which has recently been upgraded to include a drying component, too. The unit, manufactured by Alconbury Weston Ltd (UK), represents one of the few technologies available in the market for continuous API crystals isolation. The carousel is made up of multiple cylindrical ports anchored to a main rotating cylindrical body, presenting different processing stations. The crystallization

slurry is loaded into the port aligned with the first station, and is eventually discharged as dry cake after having been processed in all the stations. During operation, the stations work batchwise simultaneously, carrying out filtration, washing or drying. At every fixed time interval, the main body rotates, moving the content of each port to the following station and enabling continuous operation. Due to the rotation mechanism, the residence time in each station is the same, creating an additional challenge for process design and control. Following a quality-by-design approach, we develop a dynamic model for each processing step, and we assemble them together into the carousel model. We use multi-component macroscopic and microscopic mass, energy and momentum balances for this purpose. The developed models are connected to the upstream crystallization with suitable literature relations, linking the physical properties of the filtered cake to the CSD of the crystallization slurry (Yu *et al.*, 1996; Bourcier *et al.*, 2016). The modeling framework is then used for calculating the probabilistic design space (DS) for the isolation of aspirin from an aqueous slurry, in which a non-volatile impurity is also included. The obtained DS meets the objective of integrated design of continuous API purification, as the DS defines the probability of meeting the target critical quality attributes (CQA) of the product for all the explored combinations of critical process parameters (CPP) and feed conditions (critical material attributes, CMA). A risk-based approach (García-Muñoz *et al.*, 2015) is followed for the DS identification, accounting for model uncertainty through Monte Carlo simulations.

The rest of the manuscript is organized as follow. The carousel unit is described in Section 2, while the developed mathematical models are outlined in Section 3. The calculation of the DS for the aspirin case study is presented in Section 4, before of the concluding section.

2. THE CONTINUOUS CAROUSEL

Alconbury Weston Ltd designs and manufactures a wide variety of carousels for continuous filtration, washing and drying. The main difference across the different types of carousels concerns the volume and the overall number of the ports, which can be chosen based on the specific application. In this work we refer to a prototype (Fig. 1) made up of five ports, each with a diameter of 1 cm and maximum capacity of 10 mL, corresponding to five processing stations. All the ports are exposed to atmospheric pressure on the top. The first four stations at the bottom present a filter mesh, connected to a vacuum pump providing the pressure drop ΔP necessary for liquid and gas displacement. The slurry is loaded into the first port, where filtration is carried out. We distinguish between actual filtration, during which a slurry hold-up is still present on top of the forming cake, and cake deliquoring, which occurs after the end of filtration and consist in the mechanical displacement of the liquid retained within the cake pores. After a rotation of the carousel, in the second station a volume of wash solvent is sent on top of the cake, and eventually filtered and (partially) deliquored out. No more liquid is added in the third station, where the cake is only further deliquored. In the fourth station thermal drying is carried out through a flow of hot air. This final step is necessary to achieve the target levels of cake purity before discharge, as, due to capillary forces,

there is an equilibrium liquid concentration in the cake that cannot be eliminated through deliquoring. Finally, the dry cake is ejected from the carousel through the action of a pneumatic piston.

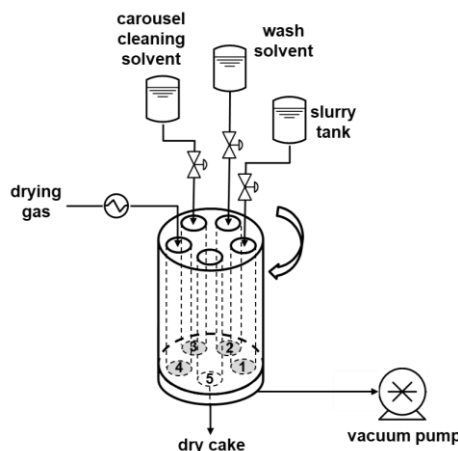


Fig. 1. The continuous carousel for integrated filtration, washing and drying. Stations 1-4 present a filter mesh at the bottom, and are connected to the vacuum pump, while station 5 is open for cake discharge.

3. MATHEMATICAL MODELING

3.1 Carousel model overview

The input/output structure of the carousel model is summarized in Fig. 2. Given a set of CMAs, CPPs and control variables (CVs), the model predicts the solvent and impurities content in the discharged cake (CQAs). The carousel model also needs the cake physical properties (such as porosity and specific resistance) as inputs. If this information is not available from experimental data, approximate values can be obtained from the slurry CSD exploiting literature models (Section 3.2). The carousel model is obtained assembling together the dynamic models of the four different processes occurring within the unit, namely *i*) slurry filtration, *ii*) cake deliquoring, *iii*) cake washing and *iv*) thermal drying. The sequence within which the processing steps occur in the physical unit is a nonlinear function of the inputs, and cannot be determined a priori. For example, a deliquoring step occurs in the first station only if the filtration duration Δt_{filt} for the particular set of inputs is smaller than the set cycle duration Δt_{cycle} . On the other hand, if a very small Δt_{cycle} is set when simulating the filtration of a slurry presenting very low filterability, filtration might end only when the cake has reached, for example, the third station, and washing will not happen in the second station. A logic-based algorithm is implemented within the carousel model to handle this issue and to call the standalone models of the processing steps mimicking the operation of the physical unit.

The models of all the processing steps are developed through differential one-dimensional balances for the reference system in Fig.3. The main assumptions common to all the models are: *i*) multiphase system (solid and liquid phases always present, gas phase present in deliquoring and drying), *ii*) multicomponent system (formed by the API, one or more solvents, and possibly additional impurities), *iii*)

homogeneous, isotropic and constant CSD and cake physical properties, *iv*) pure solid phase (composed by only the API), *v*) ideal gas behavior, *vi*) the liquid phase is an ideal solution, and *vii*) the set CMAs, CPPs and CVs do not vary during operation. Thermal drying is the only processing step considered not to be isothermal. Beside the relevant CMAs, CPPs, CVs and physical properties, all the models require the initial profiles of cake saturation S (volume of liquid in the pores over total pores volume) and of components concentration in the liquid phase as inputs, and they provide the final values of the same profiles as outputs, which become inputs to the following model. From these profiles, one can calculate and monitor the solvents and impurities content (CQAs) in every point of the cake all across carousel processing. In the following subsections, the models for the cake physical properties and the different processing steps are presented. All the models are implemented and solved in the MATLAB environment. The deliquoring and drying models are coded in C and interfaced with MATLAB through a C-MEX function to speed up the computations.

3.2 Cake physical properties models

The physical properties of a size-dispersed cake can be obtained with good approximation from the following literature relations, although experimental measurements are needed for higher accuracy. Expressing the CSD as percentage volume distribution $f(d_p)$, with respect to particle size d_p , the cake porosity ϵ (ratio between pores volume and cake volume) can be predicted by the mixture model developed by Yu et al. (1996), which also factors in the particle shape effect (the model is not reported here for sake of conciseness). The specific cake resistance α_m [m/kg] is given applying a resistance additivity hypothesis to the Kozeny-Carman model (Bourcier et al., 2016), accounting for the contribution of every bin of size d_p in the CSD to the overall resistance to the flow:

$$\alpha_m = \sum f(d_p) 180 \frac{1-\epsilon}{\epsilon^3} \frac{1}{\phi_V^2 d_p^2 \rho_s}, \quad (1)$$

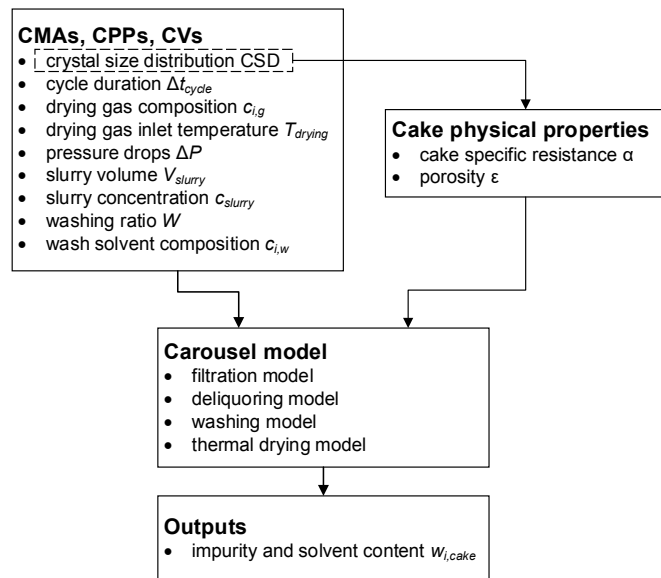


Fig. 2. Input/output structure of the mathematical model of the carousel.

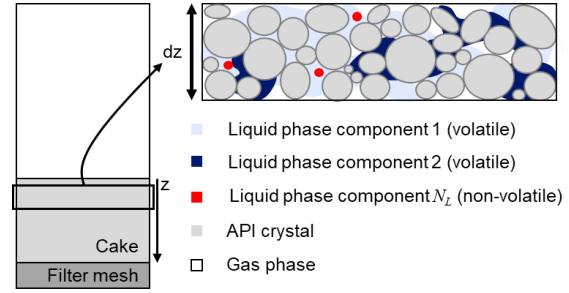


Fig. 3. Reference system of the models of the carousel processing steps. In the most general case, solid, liquid and gas phases are all present in a differential volume. The components of the liquid phase can be volatile (vaporized by thermal drying) or not.

where ϕ_V is the particle sphericity and ρ_s is the API crystals density. Cake compressibility in the carousel can be neglected, due to small cake size and the relatively low applied pressure drop. From α_m , the cake permeability k is calculated as:

$$k = \frac{1}{\alpha_m \rho_s (1-\epsilon)} \quad (2)$$

3.3 Filtration model

The solvent and impurity content in the fully saturated cake at the end of filtration are immediately obtained from the initial slurry composition, as during filtration the liquid phase composition does not vary. The significant variables to be calculated with the filtration model are Δt_{filt} , the cake height L_{cake} and the time profile of filtrate volume V . The driving force for the process ΔP is the sum of the pressure drop through the cake ΔP_{cake} and the pressure drop through the filter medium ΔP_{filter} :

$$\Delta P = \Delta P_{cake}(t) + \Delta P_{filter}(t) \quad (3)$$

Making use of the Darcy law (Muskat and Meres, 1936), (3) is rearranged to yield the instantaneous filtrate flowrate:

$$\frac{dV}{dt} = \frac{\Delta P}{\frac{\alpha_m \mu_l V_{slurry} c_{slurry}}{A^2 V_{filt, final}} + \frac{R_m \mu_l}{A}} \quad (4)$$

where V is the filtrate volume, μ_l is the liquid viscosity, A is the filter cross-section, V_{slurry} is the amount of slurry loaded in the port, c_{slurry} is the initial concentration of crystals in the slurry, R_m is the filter medium resistance and $V_{filt, final}$ is the volume of filtrate at the end of filtration, which from a mass balance is:

$$V_{filt, final} = V_{slurry} \left(1 - \frac{c_{slurry}}{\rho_s} \left(1 + \frac{\epsilon}{1+\epsilon} \right) \right) \quad (5)$$

Under the assumption of constant ΔP , (4) is integrated into the quadratic law expressing V as function of time:

$$\frac{\alpha_m \mu_l V_{slurry} c_{slurry}}{2 A^2} \frac{V^2}{V_{filt, final}} + \frac{R_m \mu_l}{A} V(t) - \Delta P t = 0 \quad (6)$$

From (4), Δt_{filt} is calculated imposing V equal to $V_{filt, final}$:

$$\Delta t_{filt} = \frac{\alpha_m \mu_l V_{slurry} c_{slurry} V_{filt, final}}{2 A^2 \Delta P} + \frac{\mu_l R_m V_{filt, final}}{A \Delta P} \quad (7)$$

At the end of filtration and during all the subsequent processing steps, L_{cake} and ΔP_{cake} correspond to, respectively:

$$L_{cake} = \frac{V_{slurry} c_{slurry}}{\rho_s(1-\epsilon)A} \quad (8)$$

$$\Delta P_{cake}(t \geq \Delta t_{filt}) = \Delta P \left(1 - \frac{R_m}{\alpha_m L_{cake} \rho_s(1-\epsilon) + R_m} \right) \quad (9)$$

3.4 Deliquoring model

During deliquoring, the liquid withheld within the pores flows out of the cake, and is replaced by the flowing-in gas phase. The fundamental cake properties for the deliquoring step are the threshold pressure P_b , above which the mechanical displacement of the cake saturation starts, and S_∞ , the cake equilibrium saturation for deliquoring. As for the other cake properties, they can be either measured or predicted. While P_b only depends on the solid physical properties, S_∞ is also affected by L_{cake} and ΔP_{cake} . Tarleton and Wakeman (2006) found a reliable relation to predict P_b , to which we apply the additivity hypothesis to account for the CSD:

$$P_b = \sum f(d_p) \frac{4.6(1-\epsilon)\sigma}{\epsilon d_p}, \quad (10)$$

where σ is the liquid surface tension. We factor the additivity hypothesis also into the established literature model for S_∞ (Tarleton and Wakeman, 2006):

$$S_\infty = \sum f(d_p) 0.155 (1 + 0.031 N_{cap}^{0.49}) \quad (11)$$

$$N_{cap} = \frac{\epsilon^3 d_p^2 (\rho_l g L_{cake} + \Delta P_{cake})}{(1-\epsilon)^2 L_{cake} \sigma}, \quad (12)$$

where N_{cap} is the capillary number and ρ_l is the liquid density. We use the Darcy law for multiphase flow (Muskat and Meres, 1936) for computing the local liquid velocity u_l :

$$u_l = -\frac{k k_{rl}}{\mu_l} \frac{dP_l}{dz}, \quad (13)$$

where P_l is the local liquid pressure, and the liquid relative cake permeability k_{rl} is obtained through (Wakeman, 1979):

$$k_{rl} = k S_R^{2+3\lambda} \quad (14)$$

$$S_R = \frac{S - S_\infty}{1 - S_\infty} = \left(\frac{P_b}{P_g - P_l} \right)^\lambda \quad (15)$$

In (14-15) the pore size distribution parameter λ is a calibration parameter for the model (usually assumed equal to 5), and P_g is the local gas pressure. P_l in (13) is calculated with (15), assuming that the gas pressure gradient is linear and constant, with total gas pressure drop through the cake equal to ΔP_{cake} , known from (9). Short-cut methods are usually resorted to in the literature for modeling the time evolution of the average cake saturation during deliquoring, while the liquid composition is assumed constant and uniform. Instead, we develop a detailed partial differential equations (PDEs) system, starting our derivation from Wakeman's early work (Wakeman, 1979). The differential total mass and species balances respectively read:

$$\frac{\partial S}{\partial t} = -\frac{1}{\epsilon} \frac{\partial u_l}{\partial z} \quad (16)$$

$$\frac{\partial c_{i,l}}{\partial t} = -\frac{u_l}{\epsilon S} \frac{\partial c_{i,l}}{\partial z}, \text{ for } i = 1, \dots, N_L, \quad (17)$$

where $c_{i,l}$ is the local liquid concentration of species, and N_L is the number of species in the liquid. The model (10-17) presents $1+N_L$ PDEs, that we semi-discretize with a high-resolution finite volume method (Van Leer, 1974) along z . The resulting ODEs are integrated with MATLAB's ode23s solver to yield the dynamic profiles of $c_{i,l}$ and S during the process.

3.5 Washing model

Cake washing is a step of utmost importance within API isolation, during which the slurry mother liquor is in major part replaced with a wash solvent. Washing is typically carried out for *i*) reducing the content of impurities (especially the non-volatile ones that cannot be eliminated through thermal drying) and *ii*) improving the drying performance with a wash solvent more volatile than the mother liquor. At the end of washing, the cake is always fully saturated. During the washing of a non pre-deliquored cake, dynamic profiles of $c_{i,l}$ are given by a species mass balance:

$$\frac{\partial c_{i,l}}{\partial t} = -\frac{u_l}{\epsilon} \frac{\partial c_{i,l}}{\partial z} - \frac{\partial}{\partial z} \left(D_{i,ax,l} \frac{\partial c_{i,l}}{\partial z} \right), \text{ for } i=1, \dots, N_L \quad (18)$$

in which $D_{i,ax,l}$ is the axial dispersion coefficient of i , which can be calculated through literature correlations or regressed from experimental data. Short-cut approaches are typically adopted in the literature for computing (18). Differently, we make use of the analytical solution of (18) found by Lapidus and Amundson (1952), reformulated in terms of washing ratio W (ratio between employed volume of wash solvent and volume of cake pores):

$$\phi_i(W, z) = \frac{c_{i,l}(W, z) - c_{i,l}(W=0, z)}{c_{i,l}(W, z=0) - c_{i,l}(W=0, z)} = 0.5 \left\{ \operatorname{erfc} \left(\frac{z/L_{cake} - W}{2\sqrt{W}} \sqrt{\frac{u_l L_{cake}}{\epsilon D_{i,ax,l}}} \right) + \exp \left(\frac{u_l z}{\epsilon D_{i,ax,l}} \right) \operatorname{erfc} \left(\frac{z/L_{cake} + W}{2\sqrt{W}} \sqrt{\frac{u_l L_{cake}}{\epsilon D_{i,ax,l}}} \right) \right\} \quad (19)$$

For a pre-deliquored cake of average saturation S_{avg} , we account for the pre-deliquoring effect on washing with a corrected washing ratio W_{corr} (Tarleton and Wakeman, 2006):

$$W_{corr} = W + 1.51(1 - S_{avg}) \exp(-1.56 \phi_i(W, z=L)) - 7.4(1 - S_{avg}^2) \exp(-1.72 \phi_i(W, z=L_{cake})) \quad (20)$$

3.6 Thermal drying model

During thermal drying, a flow of hot dry gas is sent onto the cake, to dry it below S_∞ . We calculate the local drying rate $\dot{m}_i^{L \rightarrow G}$ [kg/(m³ s)] for species i as (Burgschweiger and Tsotsas, 2002):

$$\dot{m}_i^{L \rightarrow G} = h_{M,i} a (P_{i,sat} - P_{i,g}) \eta_i, \quad (21)$$

where $h_{M,i}$ is the mass transfer coefficient (obtained from correlations or experimental data), a is the cake specific surface, which we calculate as $a = 6/d_p$ (where d_p is the Sauter diameter calculated from the CSD), and, for species i , $P_{i,sat}$ is the saturation pressure (calculated through Antoine equation), $P_{i,g}$ is the partial pressure, and η_i is a factor accounting for mass transfer limitations, mainly due to capillarity, that occur when the weight content of i in the cake $w_{i,cake}$ becomes lower than

a critical value $w_{i, \text{cake}}^{\text{crit}}$. We approximate η_i assuming it to be equal to the normalized moisture content:

$$\eta_i = \begin{cases} 1 & \text{if } w_{i, \text{cake}} \geq w_{i, \text{cake}}^{\text{crit}} \\ \frac{w_{i, \text{cake}} - w_{i, \text{cake}}^{\text{eq}}}{w_{i, \text{cake}}^{\text{crit}} - w_{i, \text{cake}}^{\text{eq}}} & \text{if } w_{i, \text{cake}} < w_{i, \text{cake}}^{\text{crit}} \end{cases}, \quad (22)$$

where $w_{i, \text{cake}}^{\text{eq}}$ is the equilibrium content of i in the cake. The differential species mass balance in the cake for the solvents and other impurities present in the liquid reads:

$$\frac{\partial}{\partial t} c_{i, \text{cake}} = -\dot{m}_i^{\text{L} \rightarrow \text{G}}, \text{ for } i=1, \dots, N_{L, \text{vol}} \quad (23)$$

where $c_{i, \text{cake}}$ is the mass concentration of i in the cake, and $N_{L, \text{vol}}$ is the number of volatile species in the liquid. For non-volatile impurities, $c_{i, \text{cake}}$ does not vary during drying, hence (23) does not need to be integrated. From $c_{i, \text{cake}}$, the local cake saturation is calculated through:

$$S = \frac{\sum_{i=1}^{N_L} c_{i, \text{cake}} / \rho_{i, l}}{\epsilon} \text{ for } i = 1, \dots, N_L, \quad (24)$$

where $\rho_{i, l}$ is the mass density of pure i in liquid form. For the $N_{L, \text{vol}}$ volatile components of the liquid phase, the species mass balance in the gas phase, in terms of mass fraction $w_{i, g}$, is:

$$\rho_g \epsilon (1-S) \frac{\partial}{\partial t} w_{i, g} = -\rho_g u_g \frac{\partial}{\partial z} w_{i, g} + \dot{m}_i^{\text{L} \rightarrow \text{G}} - w_{i, g} \sum_{i=1}^{N_L} \dot{m}_i^{\text{L} \rightarrow \text{G}}, \text{ for } i=1, \dots, N_{L, \text{vol}}, \quad (25)$$

where ρ_g is the gas density, and the gas velocity u_g is given by the Darcy law for mono-phase gas flow in a porous medium (Muskat and Meres, 1936). From experimental findings and literature correlations, inter-phase heat transfer is not limiting for the process, hence the differential energy balance for the system is developed assuming local thermal equilibrium among phases:

$$\left(\rho_s c_{p, s} (1-\epsilon) + \rho_l c_{p, l} \epsilon S + \rho_g c_{p, g} \epsilon (1-S) \right) \frac{\partial T}{\partial t} = -\sum_i (\dot{m}_i^{\text{L} \rightarrow \text{G}} \lambda_i) - u_g c_{p, g} \rho_g \frac{\partial T}{\partial z} \quad (26)$$

where $c_{p, s}$ is the solid specific heat, $c_{p, l}$ is the liquid specific heat, $c_{p, g}$ is the gas specific heat, T is the cake temperature and λ_i is the latent heat of vaporization. The model (21-26) presents $1+N_{L, \text{vol}}$ PDEs, that we semi-discretize with a first order upwind scheme. The set gas inlet composition and temperature T_{drying} (inputs of the carousel model) are used as boundary conditions for the problem. The resulting ODEs are integrated with MATLAB's ode15s solver to yield the dynamic profiles of composition and temperature of cake and gas phase during drying.

4. ASPIRIN CRYSTALS ISOLATION: DESIGN SPACE INVESTIGATION

Using the carousel model presented in Sections 3, we determine the probabilistic DS (García-Muñoz *et al.*, 2015) for the isolation of aspirin crystals with the carousel prototype described in Section 2. The liquid phase of the crystallization slurry is composed at 95%w by water, and at 5%w by a non-volatile impurity. Ethanol is used for cake washing. The maximum acceptable ethanol and impurity content in the

discharged cake is 0.5%, while water content must be below 1%. Given a fixed grid of CPPs and CMAs, for every point we calculate the probability of meeting the CQAs through a Monte Carlo simulation with 500 realizations, sampling each time the uncertain parameters of the model from their probability distributions. The CPPs of the process are identified as Δt_{cycle} and V_{slurry} , while c_{slurry} is the CMA. Extensive simulation activity showed that the CQAs are not significantly affected by major variations of W and $D_{i, ax, l}$, due to the absence of adsorption phenomena, hence they are not considered, respectively, CPPs or uncertain model parameter. A value of W equal to one is used in all the simulations, while $D_{i, ax, l}$ is obtained through literature correlations (Tarleton and Wakeman, 2006). T_{drying} and ΔP are respectively fixed at 70°C and 50 kPa. Six uncertain parameters are identified and considered in the Monte Carlo simulations (probability distributions reported in Table 1). The parameters are all sampled from a normal distribution, except for R_m , which follows a uniform distribution. During carousel operation, R_m increases due to fouling phenomena. When a threshold level of R_m is reached (maximum value of the uniform distribution), a cleaning in place procedure is carried out, and R_m is restored to its original value (minimum value of the uniform distribution). For sake of simplicity, all meshes are assumed to have the same fouling rate. A sample slurry CSD is generated and used to calculate ϵ and α_m (Section 3.2), to which an estimation error of 3% standard deviation is assumed (also accounting for CSD variability). Since during operation V_{slurry} and c_{slurry} cannot be kept completely fixed, disturbances of standard deviation 3% on their set-points for every grid point are included within the uncertain parameters. The same $h_{M, i}$ is used for water and ethanol, and a conservative estimation standard deviation of 10% is assumed, given the high variability of mass transfer phenomena. The obtained probabilistic DS is reported in Fig. 4 through two-dimensional contour plots of variable CPPs at constant c_{slurry} . When c_{slurry} increases, the surface of the feasible operative region is reduced. Through a change of variable from V_{slurry} to slurry flowrate $F_{\text{slurry}} = V_{\text{slurry}} / \Delta t_{\text{cycle}}$, the contour plots can be used for assessing the feasible operative conditions of maximum throughput.

5. CONCLUSIONS

We developed and implemented a comprehensive mathematical model of an intensified and integrated carousel for continuous filtration, washing and drying of crystallization slurries for API isolation. The model has been successfully used for determining the DS for separating aspirin crystals from an aqueous mother liquid, also containing a non-volatile impurity. Model uncertainty was accounted for during DS identification through Monte Carlo sampling from the model parameters probability distributions. Future work will involve using the model for DS identification and process optimization for other slurry systems, upon model calibration with experimental data.

ACKNOWLEDGEMENTS

Funding for this publication was made possible, in part, by the FDA through grant (U01FD006738). Views expressed in

written materials or publications and by speakers and moderators do not necessarily reflect the official policies of the Department of Health and Human Services; nor does any mention of trade names, commercial practices, or organization imply endorsement by the United States Government. F.D. gratefully acknowledges the CARIPARO Foundation for his PhD scholarship and “Fondazione Ing. Aldo Gini” for the financial support.

Table 1. Uncertain parameters for probabilistic DS calculation.

Uncertain parameter	Unit	Probability Distribution
Cake porosity ϵ	[-]	$N(0.36, 1.2E-4)$
Filter medium resistance R_m	[1/m]	$U(3E9, 6E9)$
Mass transfer coefficient h_M	[kg/(m ² s bar)]	$N(8.3E-4, 6.9E-9)$
Slurry concentration disturbance	[-]	$N(0, 9E-4 c_{slurry}^2)$
Slurry volume disturbance	kg/kg	$N(0, 9E-4 V_{slurry}^2)$
Specific cake resistance α_m	[m/kg]	$N(3.2E9, 9.2E15)$

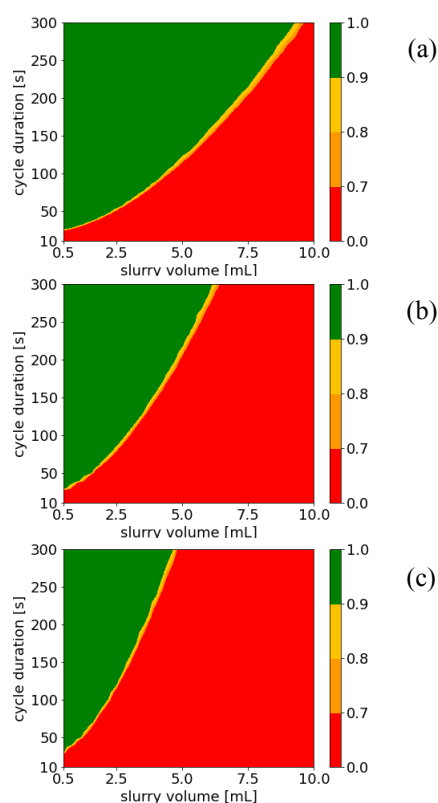


Fig. 4. The calculated robust DS, representing the probability of meeting the target CQAs. In the figures, c_{slurry} is (a) 100 kg/m³, (b) 150 kg/m³ and (c) 200 kg/m³.

REFERENCES

Benyahia, B., Lakerveld, R. and Barton, P. I. (2012) ‘A plant-wide dynamic model of a continuous pharmaceutical process’, *Industrial and Engineering Chemistry Research*, 51(47), pp. 15393–15412.

- Bourcier, D., Féraud, J. P., Colson, D., Mandrick, K., Ode, D., Brackx, E. and Puel, F. (2016) ‘Influence of particle size and shape properties on cake resistance and compressibility during pressure filtration’, *Chemical Engineering Science*, 144, pp. 176–187.
- Burgschweiger, J. and Tsotsas, E. (2002) ‘Experimental investigation and modelling of continuous fluidized bed drying under steady-state and dynamic conditions’, *Chemical Engineering Science*, 57(24), pp. 5021–5038.
- FDA, 2004. Guidance for industry, PAT-A Framework for Innovative Pharmaceutical Development, Manufacturing and Quality Assurance. <http://www.fda.gov/cder/guidance/published.html>. Accessed on 11/20/2020.
- García-Muñoz, S., Luciani, C. V., Vaidyaraman, S. and Seibert, K. D. (2015) ‘Definition of Design Spaces Using Mechanistic Models and Geometric Projections of Probability Maps’, *Organic Process Research and Development*, 19(8), pp. 1012–1023.
- Lapidus, L. and Amundson, N. R. (1952) ‘Mathematics of adsorption in beds. VI. The effect of longitudinal diffusion in ion exchange and chromatographic columns’, *Journal of Physical Chemistry*, 56(8), pp. 984–988.
- Lee, S. L., O’Connor, T. F., Yang, X., Cruz, C. N., Chatterjee, S., Madurawe, R. D., Moore, C. M. V., Yu, L. X. and Woodcock, J. (2015) ‘Modernizing Pharmaceutical Manufacturing: from Batch to Continuous Production’, *Journal of Pharmaceutical Innovation*, 10(3), pp. 191–199.
- Van Leer, B. (1974) ‘Towards the ultimate conservative difference scheme. II. Monotonicity and conservation combined in a second-order scheme’, *Journal of computational physics*, 14(4), pp. 361–370.
- Liu, Y. C., Domokos, A., Coleman, S., Firth, P. and Nagy, Z. K. (2019) ‘Development of Continuous Filtration in a Novel Continuous Filtration Carousel Integrated with Continuous Crystallization’, *Organic Process Research and Development*, 23(12), pp. 2655–2665.
- Muskat, M. and Meres, M. W. (1936) ‘The flow of heterogeneous fluids through porous media’, *Physics*. American Institute of Physics, 7(9), pp. 346–363.
- Sen, M., Rogers, A., Singh, R., Chaudhury, A., John, J., Ierapetritou, M. G. and Ramachandran, R. (2013) ‘Flowsheet optimization of an integrated continuous purification-processing pharmaceutical manufacturing operation’, *Chemical Engineering Science*, 102, pp. 56–66.
- Tarleton, S. and Wakeman, R. (2006) *Solid/liquid separation: equipment selection and process design*. Elsevier, Amsterdam (NL).
- Wakeman, R. J. (1979) ‘Low-pressure dewatering kinetics of incompressible filter cakes, I. Variable total pressure loss or low-capacity systems’, *International Journal of Mineral Processing*, 5(4), pp. 379–393.
- Wibowo, C., Chang, W. C. and Ng, K. M. (2001) ‘Design of integrated crystallization systems’, *AIChE Journal*, 47(11), pp. 2474–2492.
- Yu, A. B., Zou, R. P. and Standish, N. (1996) ‘Modifying the linear packing model for predicting the porosity of nonspherical particle mixtures’, *Industrial and Engineering Chemistry Research*, 35(10), pp. 3730–3741.